Investigation of Aluminum Foams and Graphite Fillers for Improving the Thermal Conductivity of Paraffin Wax-based Phase Change Materials

Javieradrian Ruiz, Yash Ganatra, Alex Bruce, John Howarter, and Amy M. Marconnet
Purdue University
West Lafayette, IN USA 47906
Email: marconnet@purdue.edu

ABSTRACT

Passive thermal management with phase change materials (PCMs) has become the one of the most promising methods to cool cell phone processors due to the relatively simple implementation and profound impact on processor temperatures. Enhancing the thermal properties of conventional PCMs, mainly thermal conductivity and latent heat storage, allows for an overall improved thermal management system. This study aims to improve the thermal conductivity of paraffin wax (a typical commercial PCM) by the introduction of an expanded graphite (EG) filler to form a paraffin wax composite, and then infiltration of the EG/paraffin composite into an aluminum foam matrix. The thermal conductivity of the EG/paraffin composites increases respectively to the volume percent of expanded graphite. While the thermal conductivity increased, there is some negative impact on latent heat storage compared to pure paraffin wax. The pore size of the aluminum foam matrixes also has a profound impact on both thermal conductivity and latent heat storage of the overall system. These results will allow for improvements in cooling techniques incorporated within cell phones and other mobile devices, allowing for future development of their processors (higher computational power), prolonged reliability, and longer anticipated life cycles.

KEY WORDS: Passive thermal management, Phase change materials (PCMs), Thermal conductivity enhancement, Thermal management of electronics

NOMENCLATURE

EG	expanded graphite
k	thermal conductivity, W m^{-1} K^{-1}
L	thickness, m
PCM	phase change material
T	temperature, K or ^oC
R_{th}	thermal resistance, m^2 K W^{-1}
x	position, m

Subscripts

i	layer in reference-sample-reference stack

INTRODUCTION

Electronics have become increasingly incorporated into everyday life, and are a vital component of modern society. One of the greatest limitations in developing new electronics with enhanced capabilities is the high temperatures experienced while the device is in operation. In a survey conducted by the U.S. Air Force in 1989, more than fifty percent of electronic failures were temperature related [1]. Since the time of that survey, there have been tremendous improvements in the performance and capabilities of electronics and the corresponding cooling mechanisms. Modern electronics are becoming increasingly powerful, but are also becoming increasingly compact, leading to increased heat fluxes in electronic processors. For example, in 1989 the Intel® I486-25 processor had a heat flux of approximately 3.85 W/cm^2, but by 2004 the Intel® Pentium® 4 processor 505 had a heat flux of 75 W/cm^2 [2–4]. This manifold increase in power density is a continuing trend, and must be accompanied by enhanced cooling methods if future advances in electronics are to be utilized. The thermal management of processors is vital for allowing optimum operating conditions and preventing automatic shut offs due to overheating [4]. When processors exceed a predetermined temperature threshold, damage to the processor can occur and leads to reduced future performance and reliability [4,5].

There are two general ways that devices may be cooled: active and passive cooling. Active cooling by fans or blowers would be ideal, but it is impractical in small, handheld devices as the compact size does not allow for additional components to be installed. Additionally, they add complexity and consume significant energy to function [6]. Therefore, most research currently focuses on optimizing passive cooling techniques including heat pipes [7], thermosyphons [7], heat spreaders [8], and phase change materials (PCMs) [9] in these applications. Phase change materials undergo a phase change upon heating, either a solid-solid, solid-liquid (melting), or liquid-gas (evaporation or boiling) phase change [6]. In energy storage thermal management applications, PCMs take advantage of the latent heat needed to change the phase of the material. Specifically, when phase change occurs, energy is required to break intermolecular bonds and the temperature remains relatively constant until all bonds are broken, allowing the system to operate for longer periods of time at a lower temperature [10].

Ideally a PCM would have an appropriate melting temperature (near the device safe operating temperature), high latent heat storage, and high thermal conductivity [11]. The first two criteria are already met with existing PCMs, however, those PCMs tend to have a relatively low thermal conductivity [6]. Due to this low thermal conductivity, researchers have explored many different techniques to enhance the thermal conductivity of conventional PCMs. The most straightforward method is the addition of high thermal conductivity structural fins or honeycomb structures [8,12,13]. Alternative methods include impregnating highly conductive foams with PCMs [6,8,14] and integrating several different PCMs in a coaxial structure [15,16]. One of the most effective ways to improve the thermal conductivity of PCMs is by the addition of carbon fillers and nanomaterials [10,17–20]. Inclusion of carbon fibers [17], expanded graphite [11,21,22], graphene nanoplatelets [18,23], carbon nanotubes [18], carbon

nanofibers [24], and nanomagnetite structures [19,20] in PCMs have been studied. Expanded graphite (EG) is very promising due to its relatively low cost and the formation of form stable, solid-solid transitioning PCM at a relatively low mass percent (8%, of EG) [25]. Such techniques to improve thermal conductivity through solid filler materials were developed in search of an optimal composite PCM. While some methods proved to be very effective at increasing thermal conductivity, all resulted in a composite that had a lower latent heat storage than the pure PCM utilized because of the lower percentage of material which is undergoing a phase change [9].

Here, we develop a three-part composite phase change material for improving thermal properties. Specifically, this work combines EG into paraffin wax and then the composite PCM is impregnated into aluminum foams of differing porosity. We first interrogate the thermophysical properties (thermal conductivity and latent heat), and then evaluate the impact on hot spot temperature in a system that mimics a mobile device. We demonstrate that integrating expanded graphite into paraffin wax improves thermal conductivity, however lowers its latent heat storage. The integration of all three materials (aluminum foam, expanded graphite, and paraffin wax) can severely decrease the time to reach a temperature threshold in a device that mimics that of a cellphone processor. The optimal combination of components improves the time to reach a cutoff temperature of 70°C by a factor of 2.7.

METHODS

Materials

Preparation of Composites. The EG/Paraffin wax composites are first prepared with four different volume percentages of expanded graphite (1%, 2%, 4%, and 8%). Paraffin wax with a melting temperature range of 58-62°C was acquired form Sigma-Aldrich. Expanded graphite with an average particle size of 15 μm were provided by Asbury Carbons.

The EG and paraffin wax pellets are mixed together in the solid state, then placed in an oven at 80°C until all wax fragments have melted. The mixtures are then placed in a Flaktek DAC 400 SpeedMixer™ at 2500 rpm for 30 seconds to create a homogeneous mixture. The mixed composites are heated in an oven at 80°C for 24 hours to ensure that they remain homogeneous. However, settling of the EG was observed in all samples except for the 8% volume fraction, and thus the effective volume fractions may be lower than the as prepared value.

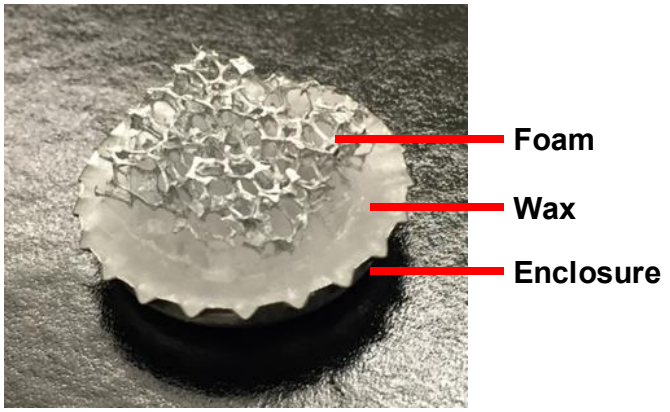

Figure 1: 10 PPI Al foam infiltrated with pure paraffin wax. The bottom enclosure, which contains the wax, is 25.4 mm diameter.

Foam Preparation. Duocel® Aluminum foams (6101 alloy) of 6-8% density were supplied by ERG Materials and Aerospace, Corp. The foams vary in pore size with the 10 pore per inch (PPI) sample having large pores and the 40 PPI sample having smaller pores. The foams are cut into small 17mm x 17mm x 12.7mm cubes to fit in the experimental fixtures.

Foam Infiltration. The foams are infiltrated with the EG/Paraffin wax composites by pouring the melted composites over the aluminum foam cubes. The foam cubes are contained in small circular containers of 25.4 mm diameter to allow for complete wax infiltration. The entire foam/container setup is allowed to cool and solidify before use in experiments (see Fig. 1). The pore sizes are sufficiently large that the wax easily infiltrates the porous foam.

As noted above, when the paraffin wax-EG composites were left in an oven for 24 hours, settling of the expanded graphite particles occurred. Therefore, during experiments, the samples must only be liquid for a short period time. The 8% composite proved to be too viscous to pour into the foam reliably and are thus not used in the device-level experiment.

Thermal Measurement Techniques

Thermal Conductivity. The thermal conductivity of the paraffin and EG/paraffin composites are measured using a miniaturized version of the reference bar method. In this technique, a sample of unknown thermal conductivity is sandwiched between two reference layers of known thermal conductivity (see Fig. 2). Aluminum adaptor plates connect the sample to the chiller (heat sink) and the heat source.

Heat conducts from the heater through the aluminum bars to the reference-sample-reference stack, and to the heat sink. Two-dimensional temperature maps are measured at the top surface of the reference-sample-reference stack. Assuming convection is negligible and when the sample and references

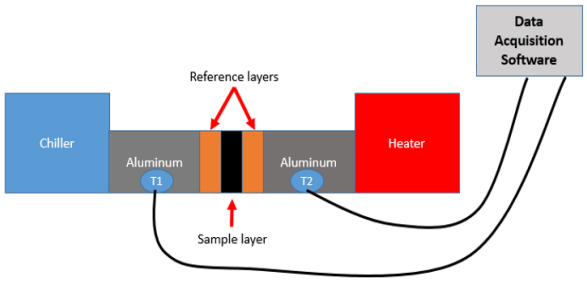

Fig 2: Schematic of thermal conductivity measurement rig. The IR microscope measures the temperature gradient in the reference-sample-reference as heat conducts from the heater, through the reference-sample-reference stack, to the chiller (heat sink). Thermocouples in the adapter plates are used to provide a reference temperature for emissivity calibration.

are the same cross-sectional area, the same heat flux (q_i'') flows through all three layers. Thus, using Fourier's law, the thermal conductivity of the sample layer is determined from the gradient in each layer:

$$k_{sample} = k_{reference} \left[\frac{dT}{dx}\right]_{reference} \Big/ \left[\frac{dT}{dx}\right]_{sample},$$

where the subscript i refers to either the reference or sample layers, k_i is the thermal conductivity of each layer, and $\left[\frac{dT}{dx}\right]_i$ is the temperature gradient extracted in each layer.

Here, the reference layers are fairly thin (~1 mm), and the sample thickness is chosen to maintain a thermal resistance on the same order of magnitude as the reference layers ($R_{th,i}=L_i/k_i$). To contain the molten material, an acrylic pocket was created from a 5mm thick acrylic plate by milling out a 1cm x 1cm x 3.175mm void in the side of the acrylic (see Fig. 3). This was done in order to prevent leakage when the wax begins to melt. The pure wax and EG/paraffin composites were then melted and poured into the pockets to be tested. Because of the required sample size, the Aluminum foams were not included in the thermal conductivity tests. The temperature profile is analyzed only near the center of the width of the sample fixture to avoid edge effects.

An IR microscope (Quantum Focus Instruments, Vista, CA) with a temperature resolution of ~0.1 K measures two-dimensional temperature map of the reference–sample-reference stack while the heat flux is applied across the sample. Thermocouples (T type, Omega), placed on the aluminum adaptor plates, monitor the temperature of both reference layers and once steady state was achieved an emissivity map is created by the IR microscope software. The emissivity map is calculated at uniform temperature of 40°C throughout the reference-sample-reference stack, and then a temperature gradient is applied across the sample (hot side of 45°C to cold side of 21°C) by use of a heater and chiller.

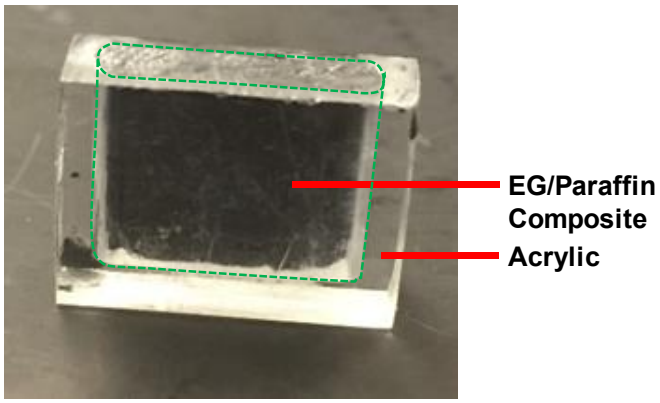

Figure 3: Acrylic pocket containing the solidified EG/paraffin composite used for thermal conductivity measurement. The acrylic serves both to contain the sample after melting and as the reference layer for measuring the heat flux. The dashed green lines show the outline of 1cm x 1cm x 3.175 mm the pocket that contains the composite material.

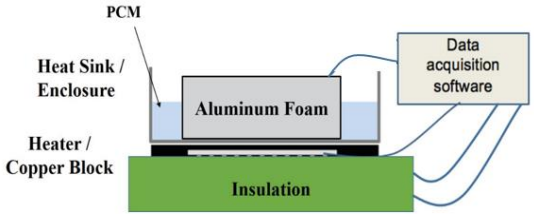

Figure 4. Schematic of the device level experimental setup. The enclosure containing the PCM and aluminum foam is directly in contact with a copper block with an embedded heater that mimics the processor during operation. Temperatures are logged by a data acquisition system at multiple locations within the system during the heating and cooling process.

Latent Heat. The latent heats of both the pure paraffin and the EG/paraffin composites are measured by a TA Instruments DSC q2000 (New Castle, DE, USA) with a liquid nitrogen cooling system. To eliminate any thermal history differences in the samples, latent heats were measured on the second heating cycle in a standard heat/cool/heat run, heating at 5°C/min from 0°C to 100°C.

Device Level Experiments. A Kapton heater and copper block are used to mimic a mobile device during operation (see Fig. 4) in order to determine the impact of the composite PCMs. The filled foams, in the circular containers, are placed on the modeled computer processor.

The 0.008" thick, 32.8 Ω Kapton heater has an outside diameter 1.5" with the heating elements contained within an inside diameter approximately 1". A 0.02" thick copper sheet, cut to the shape of the heater, is adhered with artic silver to a 40mm thick piece of firebrick (that serves as thermal insulation and is also cut to match the size as the copper plate). The Kapton heater is attached to the copper plate with the built-in epoxy backing. Another 0.02" thick copper slab covering only the heating coils (to avoid shorting out the leads to the heater) is adhered with artic silver to the top of the Kapton heater and a ¼" thick piece of copper is adhered with artic silver to the top of that copper sheet. The top ¼" piece of copper was then coated with a graphite spray to give a uniform emissivity of 0.78. A variac transformer controls the voltage supplied to the heater.

One thermocouple monitors the interior temperature of the mimicked processor along with 3 additional thermocouples to measure the temperature in the insulation and the PCM-infiltrated foam (see Fig. 4). All temperatures are recorded with a National Instruments USB-9162 data logger.

RESULTS and DISCUSSION

Effect of Expanded Graphite on the Properties of Paraffin Wax-Expanded Graphite Composites

Impact on Thermal Conductivity. The thermal conductivity of the composites, measured by the reference bar method at hot side temperature of ~45°C, increases with the addition of graphite (see Fig . 5), as expected. The uncertainty in the measurement is approximately 10% due to the uncertainty of the thermocouples used to measure the

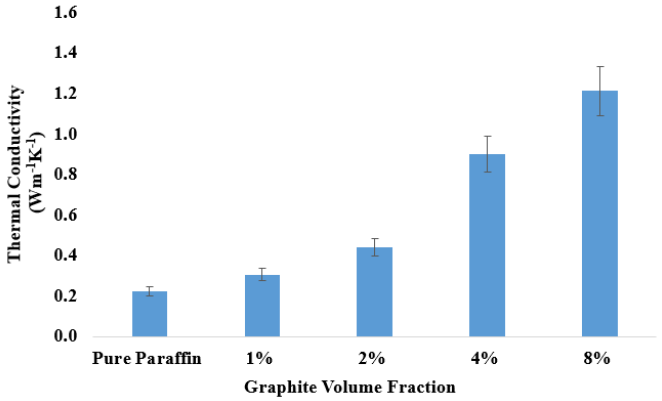

Fig. 5: Thermal conductivity of different EG/paraffin composities with increasing EG volume fraction at 45°C. Error bars show 10% error due to the uncertainy in the thermocouples used to measure the temperature during calibration and heat losses by convection at the surfaces of the sample.

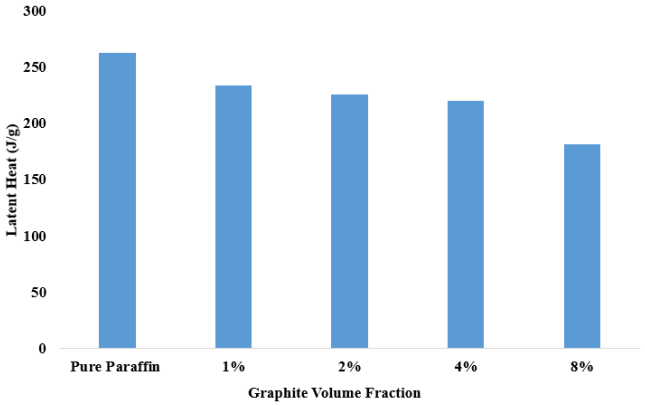

Fig. 6: Latent heats of different composites of EG/paraffin composities with increasing EG volume fraction. The heat and cooling cycles were from 0°C to 100°C with a heating and cooling rate of 5°C/min. The latent heat shown correspond to the heating curve of the DSC results.

temperature during calibration and due to heat losses by convection at the surfaces of the sample.

Impact on Latent Heat. The latent heat of the paraffin decreases with the addition of the EG (see Fig. 6) due to the volume of wax, which is replaced in the composite by EG. Since the EG does not change phase (until extreme temperatures), there is only a latent heat decrease in the composite associated with its addition

From the DSC curve, the transition temperatures and latent heats of melting associated with the paraffin wax and paraffin wax/EG composites were measured. Two peaks in the heat flow curve indicate two transition temperatures. For this paraffin wax, there appears to be a solid-solid transition around 45°C and then a solid-liquid transition around 60°C.

Impact of Foam and Expanded Graphite on Device Level Heating and Cooling Rates

Fig. 7 shows an example data trace for the temperature over time at the four locations throughout the thickness of the

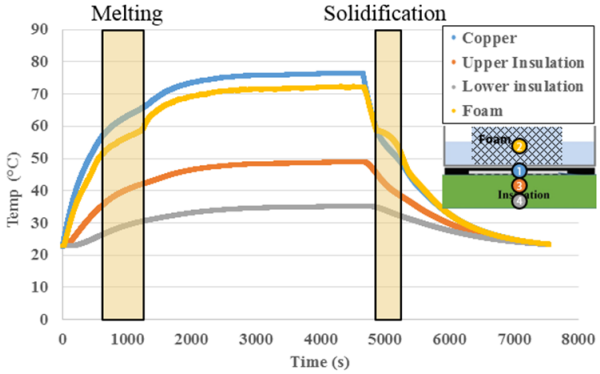

Fig. 7: Result from 10PPI and 1% expanded graphite composite

modeled processor, foam, and insulation. Note that in addition to delaying the temperature rise during heating, there is an associated elongation of the cooling time due to the solidification of the composites once the heater was switched off. This elongation of the cooling rate is due to the exothermic nature of solidification and can clearly be seen in Fig. 7 after the heater power is shut off.

The effect of the latent heat storage of all the PCMs is clearly seen in the temperature traces in Fig. 7. To directly compare the impact across different samples, we choose a metric of the time taken to reach particular cutoff temperature (see Fig. 8). This is analogous to the application in cell phones, where the processor speed is significantly throttled by the software when the temperature exceeds a set point.

Two cutoff temperatures are chosen for analysis here: 60°C (since the paraffin wax used had a melting range of 58-62°C) and 70°C (based on the maximum desired processor temperature). The PCM melts completely by 70°C. The addition of the PCMs significantly increases the time to reach both cut off temperatures, with the smaller pore size (40 PPI) foam with pure paraffin wax offering a 2 times improvement

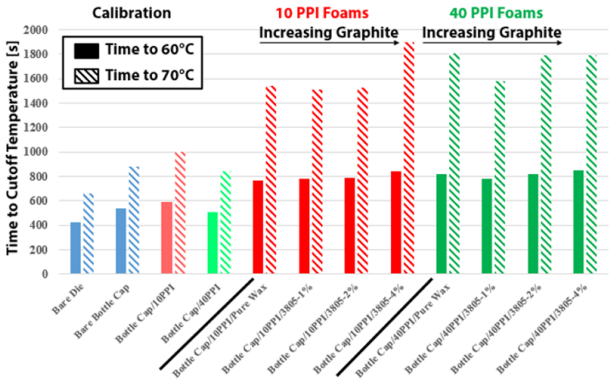

Fig. 8: Time to reach the cutoff temperature for all samples. Solid bars show the time to reach 60°C, and striped bars indicate the time to reach 70°C. For the pure wax, the foam with smaller pores (40 PPI) performed slightly better than the larger pore size foam. In the large pore foam (10 PPI) increasing graphite concentration generally improved the time to the cutoff temperature. In the smaller pore geometry, the trend with graphite is less clear.

in the time to 70°C (1800 seconds with the foam/paraffin sample as compared to 700 seconds for the bare processor die alone). For the large pore foam (10 PPI), as the percent by volume of EG increases, the time to each given cutoff temperature generally increases as well.

In this work, the optimum combination measured is the 10 PPI foam with 4% expanded graphite in the paraffin wax which demonstrated a factor of 2 increase in the time to 60°C and a factor of 2.7 increase in the time to 70°C as compared to the bare die.

CONCLUSIONS

Here we demonstrate that composite phase change materials of paraffin wax and expanded graphite infiltrated into aluminum foams significantly enhance the time to reach cutoff temperatures in devices that mimic the heat transfer in a mobile processor. Thermal property analysis show that the thermal conductivity of paraffin wax is effectively improved by the addition of expanded graphite, but it reduces the latent heat storage in the composite and these competing effects combine to impact the performance in the device level tests. These results illustrate that the three-part wax, expanded graphite, foam composites are effective for dissipating the heat and are promising for applications such as mobile electronic devices. Future work should include evaluation of the thermal cycling stability of such composite systems and optimization of properties.

ACKNOWLEDGEMENTS

This study was funded by members of the Cooling Technologies Research Center, an NSF Industry/University Cooperative Research Center at Purdue University.

REFERNCES

[1] L. T. Yeh, “Review of Heat Transfer Technologies in Electronic Equipment,” *J. Electron. Packag.*, vol. 117, no. 4, p. 333, 1995.

[2] “Intel® Pentium® 4 Processor 505/505J (1M Cache, 2.66 GHz, 533 MHz FSB) Specifications,” *Intel® ARK*, 2016. .

[3] K. Azar, “The history of power dissipation,” *Electronics Cooling*, pp. 42–50, 2000.

[4] R. Mahajan, C. P. Chiu, and G. Chrysler, “Cooling a microprocessor chip,” *Proc. IEEE*, vol. 94, no. 8, pp. 1476–1485, 2006.

[5] A. Shakouri, “Nanoscale thermal transport and microrefrigerators on a chip,” *Proc. IEEE*, vol. 94, no. 8, pp. 1613–1638, 2006.

[6] K. Lafdi, O. Mesalhy, and S. Shaikh, “Experimental study on the influence of foam porosity and pore size on the melting of phase change materials,” *J. Appl. Phys.*, vol. 102, no. 8, 2007.

[7] M. Groll, M. Schneider, V. Sartre, M. Chaker Zaghdoudi, and M. Lallemand, “Thermal control of electronic equipment by heat pipes,” *Rev. Générale Therm.*, vol. 37, no. 5, pp. 323–352, 1998.

[8] E. W. Bentilla, K. F. Sterrett, and L. E. Karre, “Research and Develpopment Study on Thermal Contril by use of Fusible Materials,” *Northrop Corp.*, 1966.

[9] B. Zalba, J. M. Marín, L. F. Cabeza, and H. Mehling, Review on thermal energy storage with phase change: materials, heat transfer analysis and applications, vol. 23, no. 3. 2003.

[10] S. Kim and L. T. Drzal, “High latent heat storage and high thermal conductive phase change materials using exfoliated graphite nanoplatelets,” *Sol. Energy Mater. Sol. Cells*, vol. 93, no. 1, pp. 136–142, 2009.

[11] A. Karaipekli, A. Sari, and K. Kaygusuz, “Thermal conductivity improvement of stearic acid using expanded graphite and carbon fiber for energy storage applications,” *Renew. Energy*, vol. 32, no. 13, pp. 2201–2210, 2007.

[12] I. M. Bugaje, “Enhancing the thermal storage of latent heat,” *Int. J. Energy Res.*, vol. 21, pp. 759–766, 1997.

[13] M. BUSBY and S. MERTESDORF, “The benefit of phase change thermal storage for spacecraft thermal management,” *22nd Thermophys. Conf.*, pp. 0–7, 1987.

[14] Y. Zhong, Q. Guo, S. Li, J. Shi, and L. Liu, “Heat transfer enhancement of paraffin wax using graphite foam for thermal energy storage,” *Sol. Energy Mater. Sol. Cells*, vol. 94, no. 6, pp. 1011–1014, 2010.

[15] J. Wang, G. Chen, and H. Jiang, “Theoretical study on a novel phase change process,” *Int. J. Energy Res.*, vol. 23, no. 4, pp. 287–294, 1999.

[16] J. Wang, Y. Ouyang, and G. Chen, “Experimental study on charging processes of a cylindrical heat storage employing multiple-phase-change materials,” *Int. J. Energy Res.*, vol. 25, no. 5, pp. 439–447, 2001.

[17] J. Fukai, M. Kanou, Y. Kodama, and O. Miyatake, “Thermal conductivity enhancement of energy storage media using carbon fibers,” *Energy Convers. Manag.*, vol. 41, no. 14, pp. 1543–1556, 2000.

[18] L. W. Fan, X. Fang, X. Wang, Y. Zeng, Y. Q. Xiao, Z. T. Yu, X. Xu, Y. C. Hu, and K. F. Cen, “Effects of various carbon nanofillers on the thermal conductivity and energy storage properties of paraffin-based nanocomposite phase change materials,” *Appl. Energy*, vol. 110, pp. 163–172, 2013.

[19] N. Sahan and H. O. Paksoy, “Thermal enhancement of paraffin as a phase change material with nanomagnetite,” *Sol. Energy Mater. Sol. Cells*, vol. 126, pp. 56–61, 2014.

[20] N. Sahan, M. Fois, and H. Paksoy, “Improving thermal conductivity phase change materials - A study of paraffin nanomagnetite composites,” *Sol. Energy Mater. Sol. Cells*, vol. 137, pp. 61–67, 2015.

[21] X. Py, R. Olives, and S. Mauran, “Paraffin/porous-graphite-matrix composite as a high and constant power thermal storage material,” *Int. J. Heat Mass Transf.*, vol. 44, no. 14, pp. 2727–2737, 2001.

[22] Y. Zhong, S. Li, X. Wei, Z. Liu, Q. Guo, J. Shi, and L. Liu, “Heat transfer enhancement of paraffin wax using compressed expanded natural graphite for thermal energy storage,” *Carbon N. Y.*, vol. 48, no. 1, pp. 300–304, 2010.

[23] H. Ji, D. P. Sellan, M. T. Pettes, X. Kong, J. Ji, L. Shi, and R. S. Ruoff, “Enhanced thermal conductivity of phase change materials with ultrathin-graphite foams for thermal energy storage,” *Energy Environ. Sci.*, vol. 7, pp. 1185–1192, 2013.

[24] A. Elgafy and K. Lafdi, “Effect of carbon nanofiber additives on thermal behavior of phase change materials,” *Carbon N. Y.*, vol. 43, no. 15, pp. 3067–3074, 2005.

[25] M. Xiao, B. Feng, and K. Gong, “Thermal performance of a high conductive shape-stabilized thermal storage material,” *Sol. Energy Mater. Sol. Cells*, vol. 69, no. 3, pp. 293–296, 2001.